Applied Surface Science 319 (2014) 339–343

Contents lists available at ScienceDirect

Applied Surface Science

journal homepage: www.elsevier.com/locate/apsusc

Effects of hydrazine hydrate treatment on the performance of reduced graphene oxide film as counter electrode in dye-sensitized solar cells

Leifei Qiu[a], Haiyan Zhang[a,b,*], Wenguang Wang[a], Yiming Chen[a,b], Rong Wang[a]

[a] School of Materials and Energy, Guangdong University of Technology, Guangzhou 510006, China
[b] Guangdong Provincial Key Laboratory of Functional Soft Condensed Mater, Guangzhou 510006, China

ARTICLE INFO

Article history:
Received 25 June 2014
Received in revised form 22 July 2014
Accepted 23 July 2014
Available online 31 July 2014

Keywords:
Hydrazine hydrate
Reduced graphene oxide
Counter electrode
Dye-sensitized solar cell

ABSTRACT

The reduced graphene oxide (RGO) counter electrodes were prepared by drop casting method and followed by heat treatment. The as-prepared RGO counter electrodes were used as substitution for Pt counter electrode in dye-sensitized solar cells (DSSCs). The effects of hydrazine hydrate in graphene oxide (GO) suspension on the performance of RGO counter electrodes were investigated. The cyclic voltammetry (CV) and electrochemical impedance spectroscopy (EIS) measurements revealed that a moderate amount of hydrazine hydrate can enhance the catalytic activity of the RGO film toward the reduction of I_3^- and decrease the sheet resistance of the film. The efficiency (η) of DSSC based on the RGO counter electrodes with optimum addition of hydrazine hydrate increased from 1.826% to 2.622% under a simulated solar illumination of 100 mW cm^{-2} (AM 1.5).

1. Introduction

Since the breakthrough work by Grätzel in 1991 and the increasing public concern about the development of new energy sources, dye-sensitized solar cell (DSSC) has attracted more and more attention because of their advantages such as low cost, simple preparation process, green material and relatively high conversion efficiencies [1–5]. Typically, a traditional DSSC is mainly composed of three parts, including a dye-sensitized nanocrystalline porous semiconductor photoanode, electrolyte and a Pt counter electrode. Although platinum can meet the main requirements of counter electrode material for DSSCs due to its high catalytic activity and good electrical conductivity, however, the high cost, limited reserve and the possibility of corroded by I_3^-/I^- redox electrolyte of Pt confine its application to a large scale [6]. Therefore, exploring non-platinum counter electrode material with low cost and high catalytic activity has important practical significance for large-scale application of DSSC.

Carbonaceous material has long been regarded as the most popular candidate for substitution of Pt due to its high electrical conductivity, heat resistance, corrosion resistance, good catalytic activity and stability for the reduction of I_3^-, abundant reserves, low cost and so on [7,8]. Carbon materials such as graphite [9], activated carbon [10], carbon black [11], carbon nanotube [6], carbon nanofiber [12] and fullerene [13] have been widely used as counter electrode materials. Since the discovery of graphene in 2004 [14], it has been considered to be the most promising carbon material for the counter electrode material of DSSC. Because the special two-dimensional honeycomb crystal structure of graphene enables it with a series of excellent performances such as larger surface area, chemical stability, high transmittance and electrical conductivity [15].

In 2008, flexible graphene film was used as electrocatalyst layer for the first time to modify the FTO counter electrode of DSSC [16]. Since then the graphene counter electrode gradually becomes the research hotspot in the field of DSSC. Jang et al. prepared graphene film on the FTO conductive glass by spin-coating method and heat treatment [17]. The DSSC with graphene counter electrode heat-treated at 350 °C achieved a highest conversion efficient of 3.6%. Zhang et al. prepared graphene nanosheets (GNs) counter electrode by screen printing technology [18], which showed a highest conversion efficiency of 2.94% after heat treatment at 450 °C. Yen et al. coated rGO films on FTO glasses by solvent-casting method followed by drying in vacuum at 120 °C overnight and the constructed DSSC showed a conversion efficiency of 2.89% [19].

However, the methods for preparing graphene counter electrode are always complex in the previous studies. In this work, we

* Corresponding author at: School of Materials and Energy, Guangdong University of Technology, Guangzhou 510006, China. Tel.: +86 20 39322572; fax: +86 20 39322572.
E-mail addresses: hyzhang@gdut.edu.cn, 9295839@qq.com, linjin2234@126.com (H. Zhang).

http://dx.doi.org/10.1016/j.apsusc.2014.07.133
0169-4332/

prepared RGO counter electrode by a simple drop-coating method using GO as precursor. The degree of GO reduction has great impact on the performance of graphene counter electrode. Hence, addition of hydrazine hydrate into the GO precursor solution and the following thermal treatment were taken to ensure proper reduction of GO to RGO. The effects of hydrazine hydrate on the structure and properties of RGO counter electrode were investigated.

2. Experimental

2.1. Preparation of RGO counter electrode

Firstly, graphite oxide was synthesized by a modified Hummer's method [20]. In detail, concentrated H_2SO_4 (92 mL), natural flake graphite (4 g), $NaNO_3$ (2 g) and potassium permanganate (12 g) was added in sequence to a 1000 mL three-neck flask which was kept in a water bath at the temperature of 3 °C. Then the mixture was stirred for 2 h at 3 and 35 °C, respectively. After that the temperature was increased to 75 °C. During the heating process, 184 mL of distilled water was dropped into the mixture. After stirring for another 15 min, a moderate of H_2O_2 (30%) was dropped into the solution until there was no gas generation. The suspension was washed and centrifuged repeatedly with distilled water until the sulfate ions could not be detected by $Ba(NO_3)_2$. The resulting product was dried in an oven at 45 °C. Secondly, 0.01 g of ethyl cellulose, 0.08 g of terpineol and 1 mL of graphite oxide aqueous solution (10 mg/mL) were added to 9 mL of absolute alcohol, and then the mixture solution was ultrasonicated for 1 h to obtain GO suspension. After that different content of hydrazine hydrate (0, 0.1, 0.2 and 0.3 mg) was added into the suspension, and the mixture was ultrasonicated for another few minutes. GO films were coated on FTO conductive glass by drop coating method and dried at a constant temperature of 25 °C. Finally, the GO films were calcined at 350 °C for 30 min under air condition to obtain RGO counter electrodes. The resulting RGO counter electrodes are named as rGO, rGO-0.1, rGO-0.2 and rGO-0.3 according to the amount of hydrazine hydrate.

2.2. Preparation of TiO_2 photoanodes and DSSCs

The commercial Degussa P25 TiO_2 (P25) was employed as the material for photoanode film. The P25 paste was fabricated according to our previously report [21]. The obtained paste was coated on clean FTO conductive glass using screen printing technique, and the thickness of film was controlled by printing times. After coating, the thin film electrode was dried at 80 °C and then sintered at 450 °C for 30 min in air. The calcined TiO_2 electrodes were immersed in 0.5 mM of N719 dye (purchased from Dalian HeptaChroma SolarTech Co., Ltd. of China) ethanol solution and kept at room temperature for 24 h. Thus, dye-sensitized TiO_2 photoanodes with thickness of ca. 11.5 μm were obtained.

Sensitized TiO_2 photoanodes and RGO counter electrodes were assembled into DSSCs by Surlyn 1702 gasket (60 μm thickness) as reported in the previous literature [21]. Then the liquid electrolyte (DHS-E23, Dalian HeptaChroma SolarTech Co., Ltd. of China) was injected into the space between the two electrodes by capillary action.

2.3. Characterizations

The surface morphology of RGO counter electrode was obtained on a ZEISS IGMA field emission scanning electron microscope. Raman spectroscopy was carried out using a Lab RAM HR 800 UV laser Raman spectroscopy. Cyclic voltammetry (CV) and electrochemical impedance spectroscopy (EIS) were measured using an electrochemical workstation (CHI660E, Shanghai Chenhua Device, China). A three-electrode system was used to test the CV curve in the voltage range of −0.7 to 1.0 V at a scan rate of 10 mV/s. A Pt electrode and an Ag/Ag^+ electrode were used as the counter and reference electrodes. The electrolyte for CV tests consists of 10 mM LiI, 1 mM I_2 and 0.1 M $LiClO_4$ in acetonitrile. The EIS measurement was carried out with two identical counter electrodes, sealing with thermoplastic hot-melt Surlyn and leaving an exposed area of 0.56 cm^{-2}. The electrolyte (also purchased from Dalian HeptaChroma SolarTech Co., Ltd. of China) was also injected into the EIS symmetric cells. The EIS tests were carried out under alternating current (AC) signal amplitude of 10 mV and frequency range from 0.01 to 10^5 Hz at 0.65 V direct current (DC) bias in the dark. The Zview software was used to fit the experimental EIS data with an equivalent circuit model.

The photocurrent–voltage characteristics of DSSCs were done on an electrochemical analyzer (CHI660C) under irradiation of 100 mW cm^{-2} (AM 1.5) from a solar simulator (Newport 91160) in ambient atmosphere. The active area of DSSCs was 0.14 cm^2.

3. Results and discussion

3.1. Morphologies and structures of counter electrodes

Fig. 1 shows the SEM images of the as-prepared RGO counter electrodes (rGO, rGO-0.1, rGO-0.2 and rGO-0.3). It can be seen from these images that compact films were uniformly formed on the FTO glass. Further observation indicates that some wrinkles exist on the surface of the films, and the number of wrinkles continuously increases with increase of hydrazine hydrate. These wrinkles increase the contact area at the interface of electrode and electrolyte, and the enlarging effective reaction area can enhance charge transfer reaction with electrolyte, thus improving the catalytic activity of RGO counter electrodes for I_3^- reduction. In addition, there was no obvious crack in the films. The close contact between RGO films and FTO glass is beneficial for electron transfer.

Raman spectroscopy is a very effective and non-destructive tool for investigating the structural variations in carbonaceous materials under different conditions. It can distinguish between disordered and ordered crystal structures according to the vibration state of the carbon atoms. Fig. 2 shows the Raman spectra of the as-prepared GO and RGO counter electrodes (rGO, rGO-0.1, rGO-0.2 and rGO-0.3). All the Raman curves have two obvious vibration peaks consisting of a D peak and a G peak. D peak corresponds to the disordered structure (sp^3) and G peak to the ordered structure (sp^2) of material, thus the integrated intensity ratio (area ratios) of D peak and G peak (I_D/I_G) can be used to evaluate the sp^2 domain size and degree of disorder of the graphene-based materials [22–26]. The I_D/I_G of GO, rGO, rGO-0.1, rGO-0.2 and rGO-0.3 were 0.81, 1.96, 2.01, 2.02 and 2.05, respectively. After reduction process, the great change of I_D/I_G indicated that the GO was successfully reduced to RGO. In addition, the I_D/I_G of RGO counter electrodes increase with the addition of hydrazine hydrate. The increase of I_D/I_G is usually the result of (a) the increase of the amount of amorphous carbon, (b) the decrease of the crystalline size and (c) higher defect density [27]. In our case, the increase of I_D/I_G is attributed to the increase of the defect density on the surface of RGO counter electrode, which can provide more active sites for reduction of I_3^- and improve the catalytic activity of RGO counter electrodes.

3.2. Electrochemical properties of counter electrodes

As we all know that the main function of counter electrode in a DSSC is providing the pathway for electron transfer from the external circuit to the redox electrolyte and catalyzing the reduction of I_3^- to promote the regeneration of dye molecules [17,28].

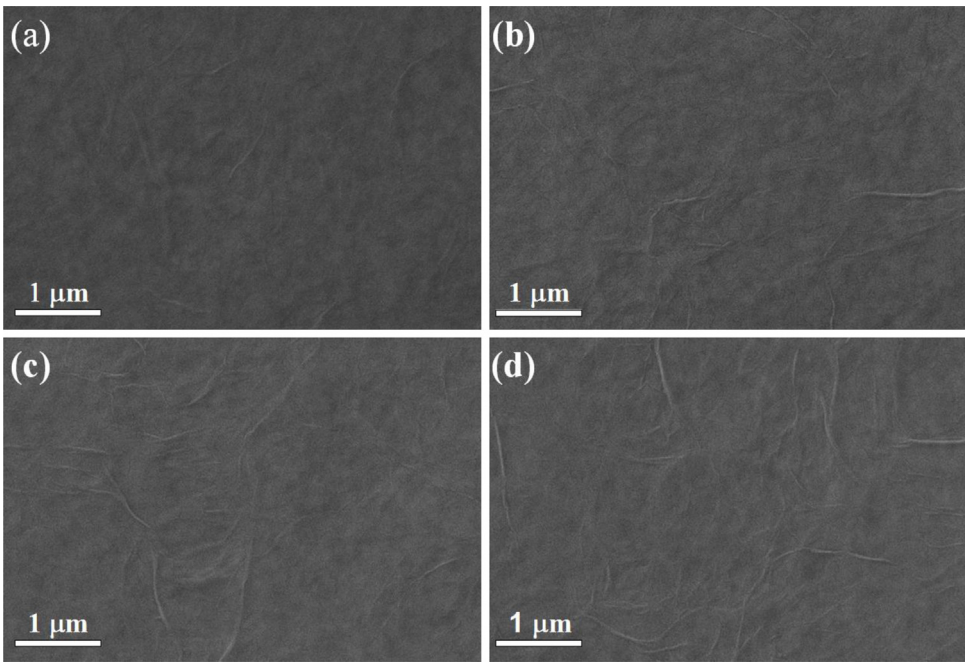

Fig. 1. FESEM images of (a) rGO, (b) rGO-0.1, (c) rGO-0.2 and (d) rGO-0.3.

Thus, the conductivity and electrocatalytic activity to the reduction of I_3^- are the key factors for determining the performance of counter electrode in a DSSC. CV is a very useful electrochemical method to study the nature, mechanism and kinetic parameters of the electrode reactions. Fig. 3 shows the CV curves of rGO, rGO-0.1, rGO-0.2 and rGO-0.3 counter electrodes. The potential of the electrodes ranges from −0.7 to 1.0 V (vs. Ag/Ag^+) at the scan rate of 10 mV s^{-1}. Two pairs of redox peaks can be observed in all of the CV curves. A_{ox} and A_{red} peaks correspond to the oxidation and reduction peaks of I_3^-/I_2, while B_{ox} and B_{red} peaks correspond to the oxidation and reduction peaks of I^-/I_3^- [29]. The reduction of I_3^- to I^- by the electrons from counter electrode is very important during the electrochemical reaction in a DSSC. Therefore, the B_{ox} and B_{red} peaks reflect the electrocatalytic properties of the counter electrodes. By comparing the reduction peaks of RGO and Pt counter electrodes, we can see that the B_{red} peaks of RGO counter electrodes are weaker than Pt counter electrode, indicating that the catalytic activity of RGO counter electrodes are relatively lower than that of Pt electrode. The electrocatalytic performance of the counter electrode in a DSSC can be evaluated by the peak current density and peak-to-peak separation (E_{pp}) of B_{ox} and B_{red} peaks. A higher peak current density and a lower E_{pp} value correspond to a better performance [30]. For the RGO counter electrodes, the E_{pp} cannot be confirmed due to weak B_{red} peaks. It can be seen from Fig. 3 that the peak current density of the RGO counter electrodes increases with the increasing addition of hydrazine hydrate, showing the improved catalytic activity of RGO counter electrodes. This result is consistent with the Raman analysis.

EIS were employed to further evaluate the catalytic activity and charge transfer process of Pt and RGO counter electrodes treated with different amount of hydrazine hydrate. Fig. 4 shows the Nyquist plots of the symmetrical cells fabricated with two identical electrodes. The Nyquist plots were modeled with an equivalent circuit (inset in Fig. 4). R_s corresponds to the high-frequency intercept on the real axis in Nyquist point and represents the series resistance of the symmetrical cells. R_{ct} represents the charge transfer resistance at the electrolyte/electrode interface for I^-/I_3^- redox reaction, and it is determined by the diameter of the high-frequency semicircle in Nyquist plot. In addition, C_1 and W_1 in the equivalent circuit represent double layer capacitor and the Nernst diffusion

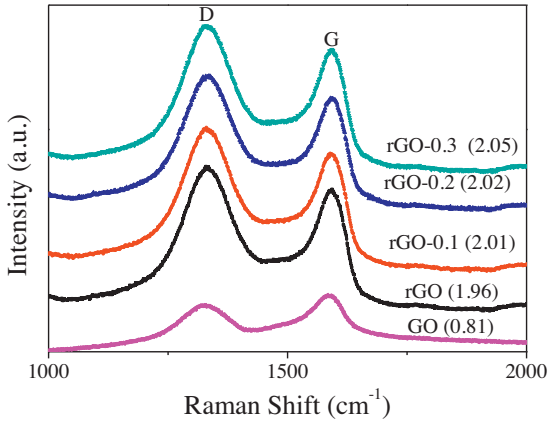

Fig. 2. Raman spectra of GO, rGO, rGO-0.1, rGO-0.2 and rGO-0.3 counter electrodes with the corresponding I_D/I_G in parentheses.

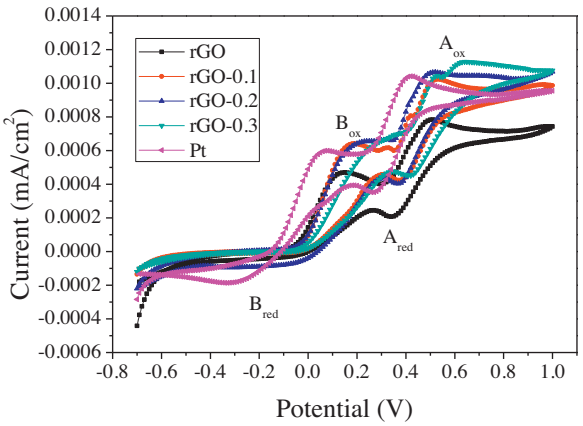

Fig. 3. Cyclic voltammograms of I^-/I_3^- redox couple of the rGO, rGO-0.1, rGO-0.2, rGO-0.3 and Pt counter electrodes.

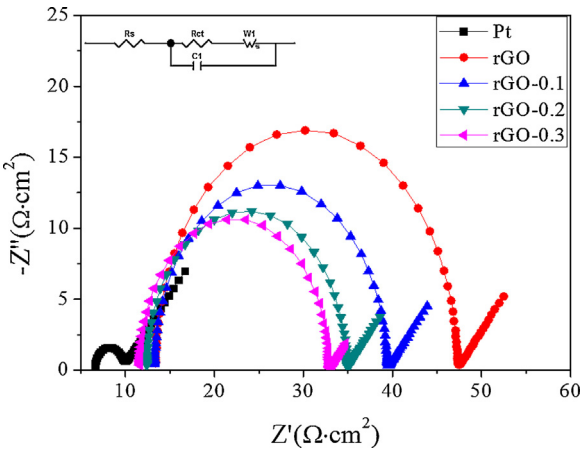

Fig. 4. Nyquist plots of the symmetrical cells fabricated with two identical counter electrodes and equivalent circuit model for fitting the resultant impedance spectra.

Table 1
Photovoltaic parameters for DSSCs fabricated with different counter electrodes.

Counter electrodes	J_{sc} (mA/cm^2)	V_{oc} (V)	FF	η (%)	R_{ct} (Ω cm^2)	R_s (Ω cm^2)
rGO	6.544	0.658	0.424	1.826	33.95	13.39
rGO-0.1	8.669	0.597	0.444	2.299	26.16	13.27
rGO-0.2	9.125	0.681	0.399	2.481	22.53	12.37
rGO-0.3	9.475	0.684	0.405	2.622	21.32	11.56
Pt	8.769	0.704	0.720	4.446	3.32	6.63

resistance of redox couple I^-/I_3^- in the electrolyte, respectively [31,32]. The R_s and R_{ct} values are listed in Table 1. It can be seen from Fig. 4 and Table 1, all the R_{ct} and R_s of RGO electrodes decrease with increasing amount of hydrazine hydrate. The decreased sheet resistance and charge transfer resistance result in the gradually improved performance of RGO electrodes. Furthermore, R_{ct} is a measure of the catalytic activity of counter electrode for reducing I_3^- [28]. Therefore, it can be revealed that with the increasing addition of hydrazine hydrate, the catalytic activity of RGO counter electrodes for reducing I_3^- would be enhanced, which is in consonance with the CV results.

3.3. Photovoltaic performance of DSSCs

Fig. 5 displays the *J–V* curves of P25 based DSSCs with various counter electrodes of rGO, rGO-0.1, rGO-0.2, rGO-0.3 and Pt under a simulated solar illumination of 100 mV cm^{-2} (AM 1.5). The

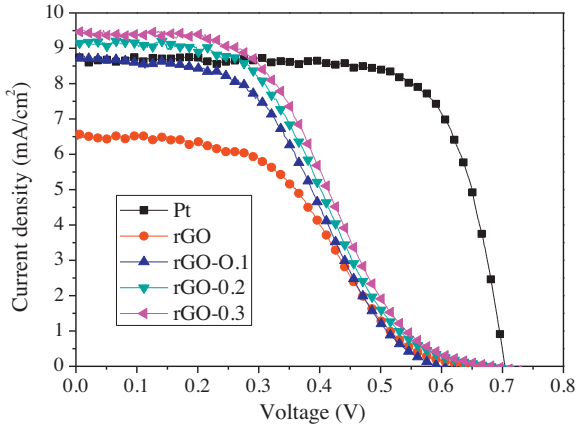

Fig. 5. *J–V* curves of DSSCs based on the rGO, rGO-0.1, rGO-0.2, rGO-0.3 and Pt counter electrodes.

photovoltaic parameters of the DSSCs such as short-circuit photocurrent density (J_{sc}), open-circuit voltage (V_{oc}), fill factor (FF) and power conversion efficiency (η) are listed in Table 1. The J_{sc} and η of the RGO counter electrodes increased with increasing amount of hydrazine hydrate. The η raises from 1.826% to 2.622%. The improved conversion efficiency of the DSSCs can be attributed to the larger active surface-area, lower sheet resistance and higher catalytic activity of the RGO counter electrodes pretreated with hydrazine hydrate, which is advantageous for increasing the I^-/I_3^- redox reaction rate on the counter electrode, thus increasing the J_{sc} and η [33].

4. Conclusion

The RGO counter electrodes were prepared by drop casting method with addition of hydrazine hydrate and following by heat treatment at 350 °C. The as-prepared RGO counter electrodes were used as substitution for Pt counter electrode in DSSCs. Results obtained from SEM images and Raman spectra show that the addition of hydrazine hydrate can improve the surface area and defect density on the surface of RGO counter electrodes, which is beneficial for improving the catalytic activity of RGO counter electrodes. Furthermore, CV and EIS results confirmed that the sheet resistance decreases with increasing addition of hydrazine hydrate. The η of DSSCs based on the RGO counter electrodes with 0.3 mg of hydrazine hydrate (2.62%) was 43.2% higher than that of RGO counter electrode without hydrazine hydrate (1.83%). Although the performance of DSSCs based on the RGO counter electrodes is still lower than DSSC based on the Pt counter electrode, it has great potential to be used as counter electrode in DSSCs due to its unique crystal structure, good electrical conductivity, and chemical stability and so on.

Acknowledgments

This work was supported by the National Natural Science Foundation of China (Nos. 51276044 and 51302043) and the China Postdoctoral Science Foundation (2014M550429).

References

[1] B. O'Regan, M. Gratzel, Low-cost high-efficiency solar cell based on dye-sensitized colloidal TiO_2 films, Nature 353 (1991) 737–740.
[2] W.G. Wang, H.Y. Zhang, R. Wang, F. Ming, Y.M. Chen, Design of a TiO_2 nanosheet/nanoparticle gradient film photoanode and its improved performance for dye-sensitized solar cells, Nanoscale 6 (2014) 2390–2396.
[3] J.J. Fan, S.W. Liu, J.G. Yu, Enhanced photovoltaic performance of dye-sensitized solar cells base on TiO2 nanosheets/graphene composite films, J. Mater. Chem. 22 (2012) 17027–17036.
[4] J.G. Yu, J.J. Fan, K. Lv, Anabases TiO_2 nanosheets with exposed (0 0 1) facts: improved photoelectric conversion efficiency in dye-sensitized solar cells, Nanoscale 2 (2010) 2144–2149.
[5] J.G. Yu, Q.L. Li, J.J. Fan, B. Cheng, Fabrication and photolytic performance of hierarchically titan ate tubular structures self-assembled by nanotubes and nanosheets, Chem. Commun. 47 (2011) 9161–9163.
[6] D.W. Zhang, X.D. Li, S. Chen, Z. Sun, X.J. Yin, S.M. Huang, Performance of dye-sensitized solar cells with various carbon nanotube counter electrode, Microchim. Acta 174 (2011) 73–79.
[7] R. Bajpai, S. Roy, N. Koratkar, D.S. Misra, NiO nanoparticles deposited on graphene platelets as a cost-effective counter electrode in a dye sensitized solar ell, Carbon 56 (2013) 56–63.
[8] W.Y. Cheng, C.C. Wang, S.Y. Lu, Graphene aerobes as a highly efficient counter electrode material for dye-sensitized solar cell, Carbon 54 (2013) 291–299.
[9] X.M. Feng, X.W. Huang, Z. Tan, B. Zhao, S.T. Tan, Application research of polypyrrole/graphite composite counter electrode for dye-sensitized solar cells, Acta Chim Sin. 69 (6) (2011) 653–658.
[10] J.K. Chen, K.X. Li, Y.H. Luo, X.Z. Guo, D.M. Li, M.H. Deng, A flexible carbon counter electrode for dye-sensitize solar cells, Carbon 47 (2009) 2704–2708.
[11] K. Imoto, K. Takahashi, T. Yamaguchi, T. Komura, J. Nakamura, K. Murata, High-performance carbon counter electrode for dye-sensitized cells, Sol. Energy Mater. Sol. cells 79 (2003) 459–469.

[12] D. Sebastian, V. Baglio, M. Girolamo, R. Moliner, M.J. Lazaro, A.S. Arico, Carbon nanofiber-based counter electrode for low cost dye-sensitized solar cells, J. Power Sources 250 (2014) 242–249.
[13] T. Hino, Y. Ogawa, N. Kuramoto, Preparation of functionalized and non-functionalized fullerene thin films on ITO glasses and the application to a counter electrode in a dye-sensitized solar cell, Carbon 44 (2006) 880–887.
[14] K.S. Novoselov, A.K. Geim, S.V. Morozov, D. Jiang, Y. Zhang, S.V. Dubonos, I.V. Grigorieva, A.A. Firsov, Electric field effect in atomically thin carbon films, Science 306 (2004) 666–669.
[15] G. Venugopal, K. Krishnamoorthy, S.J. Kim, An investigation on high-temperature electrical transport properties of graphene-oxide nano-thin films 280 (2013) 903–908.
[16] Y.X. Xu, H. Bai, G.W. Lu, C. Li, G.Q. Shi, Flexible graphene films via the filtration of water-soluble no covalent functionalized graphene sheets, J. Am. Chem. Soc. 130 (2008) 5856–5857.
[17] H.S. Jang, J.M. Yun, D.Y. Kim, D.W. Park, S.I. Na, S.S. Kim, Moderately reduced graphene oxide as transparent counter electrodes for dye-sensitized solar cells, Electrochim. Acta 81 (2012) 301–307.
[18] D.W. Zhang, X.D. Li, S. Chen, H.B. Li, Z. Sun, X.J. Yin, S.M. Huang, Graphene nanosheet counter-electrodes for dye-sensitized solar counter electrodells, 2010 3rd International Nanoelectronics Conference (INEC) 1 and 2 (2010) 610–611.
[19] M.Y. Yen, C.C. Teng, M.C. Hsiao, P.I. Liu, W.P. Chuang, C.C.M. Ma, et al., Platinum nanoparticle/graphene composite catalyst as a novel composite counter electrode for high performance dye-sensitized solar cells, J. Mater. Chem. 21 (2011) 12880–12888.
[20] Z.D. Huang, H.Y. Zhang, Y.M. Chen, W.G. Wang, Y.T. Chen, Y.B. Zhong, Microwave-assisted synthesis of functionalized graphene on Ni foam as electrode for supercapacitor application, Electrochim. Acta 108 (2013) 421–428.
[21] H.Y. Zhang, W.G. Wang, L. Hui, R. Wang, Y.M. Chen, Z.W. Wang, Effects of TiO_2 film thickness on photoltaic properties of dye-sensitized solar cell and its enhanced performance by graphene combination, Mater. Res. Bull. 49 (2014) 126–131.
[22] J.X. Wu, H. Xu, J. Zhang, Raman spectroscopy of graphene, Acta Chim. Sin. 72 (2014) 301–318.
[23] Y.H. Yang, H.J. Sun, T.J. Peng, Q. Huang, Synthesis and structural characterization of graphene-based membranes, Acta Phys. Chim. Sin. 27 (3) (2011) 736–742.
[24] K. Bogdanov, A. Fedorov, V. Osipov, T. Enoki, K. Takai, T. Hayashi, V. Ermakov, S. Moshkalev, A. Baranov, Annealing-induced structural changes of carbon onions: high-resolution transmission electron microscopy and Raman studies, Carbon 73 (2014) 78–86.
[25] Y.J. Jeon, J.M. Yun, D.Y. Kim, S.I. Na, S.S. Kim, Moderately reduced graphene oxide as hole transport layer in polymer solar cells via thermal assisted spray process, Appl. Surf. Sci. 296 (2014) 140–146.
[26] V. Singh, D. Joung, L. Zhai, S. Das, S.I. Khondaker, S. Seal, Graphene based materials: past, present and future, Prog. Mater. Sci. 56 (2011) 1178–2127.
[27] P. Hasin, M.A. Alpuche-Aviles, Y.Y. Wu, Electrocatalytic activity of graphene multilayer toward I^-/I_3^-: effect of preparation conditions and polyelectrolyte modification, J. Phys. Chem. C 114 (37) (2010) 15857–15861.
[28] T. Battumur, S.H. Mujawar, Q.T. Truong, S.B. Ambade, D.S. Lee, W. Lee, S.H. Han, S.H. Lee, Graphene/carbon nanotube composite as a counter electrode for dye-sensitized solar cells, Curr. Appl. Phys. 12 (2012) e49–e53.
[29] T.L. Zhang, H.Y. Chen, C.Y. Su, D.B. Kuang, A novel TCO- and Pt-free counter electrode for high efficiency dye-sensitized solar cells, J. Mater. Chem. A 1 (2013) 1724–1730.
[30] W. Wei, H. Wang, Y.H. Hu, Unusual particle-size-induced promoter-to-posion transition of ZrN in counter electrodes for dye-sensitized solar cells, J. Mater. Chem. A 1 (2013) 14350–14357.
[31] F. Gong, X. Xu, Z.Q. Li, G. Zhou, Z.S. Wang, NiSe2 as a efficient electrocatalyst for a Pt-free counter electrode of dye-sensitized solar cells, Chem. Commun. 49 (2013) 1437–1439.
[32] G.T. Yue, J.H. Wu, Y.M. Xiao, J.M. Lin, M.L. Huang, Z. Lan, L.Q. Fan, Functionalized graphene/poly(3, 4-ethylenedioxythiophene):polistyrensulionate as counter electrode catalyst for dye-sensitized solar cells, Energy 54 (2013) 315–321.
[33] G.T. Yue, J.H. Wu, J.Y. Lin, Y.M. Xiao, S.Y. Tai, J.M. Lin, M.L. Huang, Z. Lan, A counter electrode of multi-mall carbon nanotubes decorated with tungsten sulfide used in dye-sensitized solar cells, Carbon 55 (2013) 1–9.